IEEE Access
Multidisciplinary | Rapid Review | Open Access Journal

Received January 8, 2020, accepted February 1, 2020, date of publication February 5, 2020, date of current version February 17, 2020.

Digital Object Identifier 10.1109/ACCESS.2020.2971772

Trajectory Optimization for Cellular-Enabled UAV With Connectivity Outage Constraint

YU-JIA CHEN, (Member, IEEE), AND DA-YU HUANG
Department of Communication Engineering, National Central University, Taoyuan City 320, Taiwan
Corresponding author: Yu-Jia Chen (yjchen@ce.ncu.edu.tw)

This work was supported by the Ministry of Science and Technology (MOST) in Taiwan under Grant MOST 108-2218-E-008-016-MY2.

ABSTRACT This paper studies the trajectory optimization problem of a single cellular-enabled unmanned aerial vehicle (UAV), taking into account the outage performance of the entire trajectory. To provide real-time control, it is critical for UAV to maintain reliable connectivity with the ground base station (GBS). We first consider the connectivity outage performance, which is defined as the sum of the time duration of the outage performance not meeting a predefined threshold during the entire UAV mission. Then we formulate a trajectory optimization problem to minimize the mission completion time, while ensuring a sum constraint of the connectivity outage performance. We show that the connectivity outage constraint can be transformed into a flying area constraint. Since the formulated problem is NP-hard, a low-complexity method is proposed to solve the problem by finding the shortest path in an undirected weighted graph with enlarged GBS coverage. Simulation results demonstrate the superiority of the proposed scheme over other state-of-the-art schemes, in terms of trajectory length and computational complexity.

INDEX TERMS Unmanned aerial vehicle (UAV), trajectory optimization, cellular networks.

I. INTRODUCTION

Unmanned aerial vehicles (UAVs) have recently gained wide popularity in various transportation and sensing applications [1]. For example, the UAVs can be used for package delivery or act as a mobile data collector to gather the information from the sink nodes [2]. To support many use cases of UAVs in beyond visual line-of-sight (LOS) scenarios, 3GPP has approved the study item [3] on enhancing the existing cellular networks for UAVs (i.e., cellular-enabled UAVs). In this case, the wireless communication between UAVs and ground base station (GBS) plays a critical role in the control and safety of the UAV system [4].

To support safety-critical control, the trajectory design of cellular-enabled UAVs should consider the following aspects. First, maintaining reliable wireless connectivity between UAVs and GBS is one the key objectives as discussed in 3GPP [5]. Recent studies have shown that the outage capacity of air-to-ground links is less than that of air-to-air links due to longer average link length [6]. However, it still requires further investigation on trajectory design considering an underlying cellular network and its impact on outage performance [7]. Second, since carrying sensors or package can significantly reduce the battery life, the flight duration of the existing UAV systems is at most from 10 to 20 minutes [8]. Given the limited flight duration, the flight efficiency of UAVs requires careful consideration.

In the literature, the UAV trajectory design has been studied for various wireless systems, such as UAV-enabled mobile networks [9]–[12], privacy-preserving communications [13]–[18], UAV-assisted mobile edge computing [19]–[21], and UAV-assisted sensor networks [22], [23]. Similar to this work, the authors in [24], [25] have studied the trajectory design problem for cellular-enabled UAVs aiming to minimize the mission completion time. Since the coverage area of multiple GBSs commonly becomes an irregular polygon, it is a challenging task to find the optimal UAV trajectory. In [24], the authors proposed a graph theory based method to find the shortest trajectory based on the Dijkstra algorithm. The authors in [25] further considered the problem of finding the shortest path during which the UAV can maintain its cellular connection more than a given time constraint. Such constraint is critical for the safety functionalities of UAV systems, such as exchanging remote control commands. However, the impact of different altitudes of GBS on the coverage area has not been considered in these works, which assume that all the GBS are located at the same altitude. Moreover, these works considered only the path loss and ignored the

The associate editor coordinating the review of this manuscript and approving it for publication was Wei Wang.

fading characteristics of the wireless channel. To the best of our knowledge, we are the first to incorporate the outage constraint in Rayleigh fading environment into the UAV trajectory design problem.

In this paper, we consider the UAV trajectory design problem in which, given a start and an end point, our goal is to minimize the mission completion time by finding the optimal UAV trajectory subject to the *connectivity outage* constraint. The connectivity outage is defined as the time duration of the outage performance not meeting a predefined threshold during the entire UAV mission. By introducing the connectivity outage constraint, the outage performance of aerial channel and the connectivity performance of the entire trajectory can be guaranteed simultaneously. This is a new design framework that needs to jointly consider the trajectory length and the distance from the serving GBS. It must be pointed out that we focus on the downlink transmission (i.e., ground-to-air mode) as in [24], [25], which is critical for the UAV to receive the control packets from the GBS. Also, here we do not consider the uplink transmission (i.e., air-to-ground mode) and the power control of UAVs.

Intuitively, to minimize the mission completion time, the UAV should fly straight to the end point. However, it is almost impossible that the UAV is covered by at least one GBS during the whole trajectory, especially in rural areas where drone delivery is highly desired. Thus, the communication-aware trajectory design needs to find an optimal balance between the link reliability and trajectory length. The contributions of this paper are multi-fold:

- We formulate a trajectory optimization problem with the connectivity outage constraint. Then, we show that the connectivity outage constraint can be transformed into a flying area constraint which can be viewed as the maximum allowable distance between the UAV and its associated GBS. Hence, the formulated problem is a generalization of the trajectory design problem with zero outage constraint. We prove that the formulated problem is NP-hard by a reduction from the obstacle-removing shortest path problem.
- We analyze the formulated problem in a simple case with three GBSs. By hypothetically extending the coverage area of some GBSs, we show that the intersection point of the coverage boundaries is the key to obtaining the optimal trajectory. Based on this observation, we characterize the optimal tradeoff between link reliability and trajectory length.
- We propose a greedy algorithm to get an approximate optimal solution by finding the shortest path in an undirected weighted graph with enlarged GBS coverage. Our results demonstrate that the proposed scheme can find an approximate optimal trajectory with low computational complexity.

The rest of this paper is organized as follows. Section II reviews related works regarding the trajectory design of UAVs. The system model and problem formulation are described in Section III. In Section IV, we analyze the problem and prove its NP-hardness. In Section V, the optimal tradeoff between link reliability and trajectory length is provided and the greedy algorithm is proposed for designing the UAV trajectory. Simulation results are discussed and analyzed in Section VI. Finally, we conclude this paper in Section VII.

II. RELATED WORK

Recently, many research contributions in UAV trajectory optimization aim to find the optimal trajectory considering wireless communication performances. Existing works can be classified into two categories: UAV-assisted communications and cellular-enabled UAV communications.

A. UAV-ASSISTED COMMUNICATIONS

Since traditional GBSs suffer from limited coverage capabilities, UAV assisted-communications have received a significant amount of attention in recent years. In UAV assisted-communications, UAV can be used as flying base stations to extend the wireless coverage of the cellular networks. Due to the shortened communication distance, it is expected to achieve higher throughput and lower latency as compared to terrestrial communications.

In [26], the authors designed the shortest trajectory for which the UAV transmits the file to multiple ground terminals. UAV is deployed to act data collector for prolonging the lifetime of energy-limited devices [2]. In [27], the authors designed UAV trajectory for collecting all the information sent by ground nodes in the Rician fading channel. Another line of works consider deploying UAVs as flying base stations [9], [10], [28]–[30]. In [29], a new design paradigm of jointly considered the UAV trajectory and the communication throughput was proposed based on machine learning. The work in [9] optimized the trajectories of multi-UAVs for maximizing throughput. Since the communication delay is directly affected by the distance between two neighbor UAVs, the authors of [10] proposed an UAV trajectory optimization method to reduce the delay in multi-UAV networks. Also, UAV can be utilized as a mobile relay to forward data [4]. The authors of [11] proposed an UAV mobile relaying technique which assists cellular networks to maximize throughput. The work in [31] proposed an iterative algorithm which maximizes the sum rate of UAV-served edge users by optimizing UAV trajectory. In [19], the authors proposed to utilize UAVs to offload the data to the selected GBS. The UAV trajectory was designed to minimize the mission completion time. In [20], the UAV-based mobile cloud computing system was deployed to provide offloading opportunities to mobile devices. The flight trajectory of a single UAV was designed, where the bit allocation and the energy consumption of UAVs were taken into account. The work in [21] studied a UAV-aided mobile edge computing system to provide computation offloading services for ground users. To maximize the sum bits offloaded from all users, the authors jointly optimized user association, UAV trajectory, and transmission power of each user.

B. CELLULAR-ENABLED UAV COMMUNICATIONS

In cellular-enabled UAV communications, the UAV acts a user equipment (i.e., UAV-UE) which is served by the GBS [32]. In particular, integrating UAVs into cellular networks may cause uplink interference to neighbor GBS due to the increase of the probability of having LOS links with GBS. The authors of [33] investigated the performance of aerial radio connectivity considering the interference effects in a typical rural area. In [32], a machine learning based power control and cell association method was proposed to reduce the communication delay between UAVs and GBS. Besides, the UAV transmissions are vulnerable to eavesdropping attack due to its dominant LOS propagation in broadcast channels [34]. Considering a potential eavesdropper on the ground, the authors of [35] proposed a low-complexity algorithm to jointly design the UAV trajectory and the transmit power. Other works considering security and privacy in UAV communication networks were presented in [13]–[17]. In [13], the authors optimized the altitude of UAV to maximize the secrecy rate without eavesdropper location information. The authors of [14] considered the scenario where a UAV is operated to capture images while maintaining the privacy of the ground users. The flight trajectory was designed to minimize mission completion time with no privacy of sensitive area being violated. The work in [15] considered a covert communication problem in UAV networks. To hide the wireless transmission between UAVs, the authors jointly optimized the UAV transmit power and flight trajectory. The authors in [16] proposed a privacy protection scheme for location data in the Internet of drones. In [17], a machine learning based attack in UAV-based wireless networks was investigated.

Since the flight time of UAV is limited by the battery, some research works have been proposed for minimizing UAV mission completion time by optimizing its trajectory. Given a start point and an end point, the authors of [24] proposed a graph method which utilizes the Dijkstra algorithm to find the shortest path while ensuring that it is always connected with at least one GBS. A similar problem is addressed in [25], in which the UAV is allowed to lose connectivity with the GBS in a tolerable time. However, the works in [24], [25], [36] ignored the fading effect of the wireless channel, which is an essential feature in aerial communications. Also, only the LOS component between the UAV and the GBS was considered in these works. In this paper, we further consider both non-line-of-sight (NLOS) and LOS components in the channel model as in [37]. In essence, the radio propagation experienced by cellular-connected UAVs is affected by the relative altitude between the UAV and the GBS.

Compared to [24], [25], we further investigate the trajectory optimization problem by introducing a connectivity constraint which ensures the outage performance during the entire UAV mission. Then, a maximum allowable distance between the UAV and GBS is derived considering the altitude of UAV and GBS. We prove that the formulated problem is NP-hard and thus cannot be solved by classical deterministic shortest path algorithms (such as Dijkstra). Also, we show that the model considered in [24] is a special case of our problem.

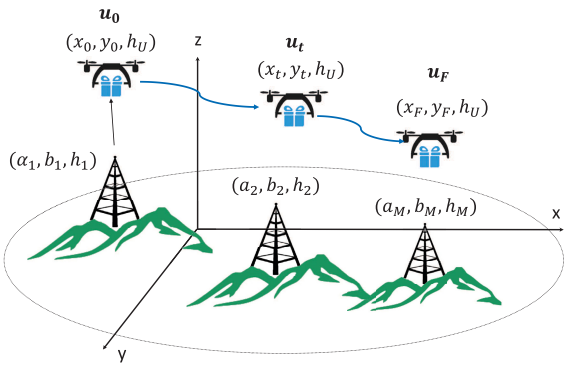

FIGURE 1. Cellular-enabled UAVs with GBSs at different altitudes.

TABLE 1. List of Notations.

Symbol	Description
u_0, u_F	UAV start and end point
T	Mission completion time
u_t	UAV coordinate at time t, t $\in [0, T]$
g_m	The mth GBS coordinate, $m \in \mathbb{M}$
d_m	The distance between UAV and the mth GBS
P_{LOS}, P_{NLOS}	LOS and NLOS probability
Pw	The transmit power of GBS
PL_m	Path loss between UAV and the mth GBS
β_0	Channel power gain at the reference distance of 1 m
ρ	Small-scale channel fading from GBS to UAV
σ^2	Noise power spectral
γ_t	The received SNR of UAV
R	Connectivity outage ratio
h_U	UAV altitude
$V_{\max}$	The maximum UAV speed

III. SYSTEM MODEL AND PROBLEM FORMULATION

In this section, we describe the cellular-enabled UAV trajectory model and the channel model between UAV and GBS. Then, the problem on optimal trajectory of the UAV is mathematically formulated.

A. UAV TRAJECTORY MODEL

As shown in Fig. 1, we consider a single UAV that moves within an area consisting of M GBSs. We assume that the GBSs are allocated with orthogonal spectrum and thus there is no interference to the GBS-UAV communications. We refer to $\mathbb{M} = \{1, \ldots, M\}$ as the set of GBSs. The UAV is designated to fly from a predetermined start point $u_0 = (x_0, y_0, h_U)$ to an end point $u_F = (x_F, y_F, h_U)$ with constant speed $V_{\max}$ at a fixed altitude h_U. We denote $g_m = (a_m, b_m, h_m)$ as the coordinate of the mth GBS in a three-dimensional coordinate system, where h_m represents the altitude of the mth GBS. Assume that the UAV altitude is higher than that of every GBS, i.e., $h_U > h_m, m \in \mathbb{M}$. The time-varying coordinate of the UAV is denoted as $u_t = (x_t, y_t, h_U), t \in [0, T]$, where T is mission completion time depending on the trajectory length.

Denote S as the total number of the flight direction changes in a mission. Let u^s be the point at which the UAV changes the sth direction. Also, we have $u^0 = u(0) = u_0$ and $u^S = u(T) = u_F$, where u^S represents the UAV's arrival at the end point. Thus, the UAV trajectory can be expressed as a sequence of points $P = \{u^0, \ldots, u^S\}$. The mission completion time can be expressed as

$$T = \frac{\sum_{i=1}^{S} \left\| u^i - u^{i-1} \right\|}{V_{\max}}. \tag{1}$$

B. CHANNEL MODEL

The distance between the UAV and the mth GBS at time instant t is given by

$$d_m(t) = \|u_t - g_m\|, \quad m \in \mathbb{M}, \tag{2}$$

where $\|\cdot\|$ denotes the Euclidean norm operation. Let Pw denote the transmit power of GBS, and β_0 denote the channel power gain at the reference distance $d_0 = 1$ m. We define $\gamma_0 \triangleq \frac{W \cdot \beta_0}{\sigma^2}$ as the reference signal-to-noise ratio (SNR) at 1 m, where σ^2 is the additive white Gaussian noise (AWGN) power. The maximum received SNR γ_t of the UAV at time t can be expressed as [38]

$$\gamma_t = \frac{Pw \cdot \max_{m \in \mathbb{M}} |h_m(t)|^2 \cdot PL_m(t)}{\sigma^2}, \tag{3}$$

where $PL_m(t)$ is the path loss between UAV and the mth GBS at time t and $|h_m(t)|^2$ is the channel gain between the mth GBS and UAV at time t, i.e.,

$$|h_m(t)|^2 = \beta_0 \times \rho^2, \tag{4}$$

where ρ^2 is an exponential random variable with unit mean accounting for the small-scale Rayleigh fading.

The wireless channel between GBSs and UAV can be parameterized by two cases: LOS and NLOS cases. Therefore, $PL_m(t)$ can be written as

$$PL_m(t) = P_{LOS,m}(t) \times PL_{LOS,m}(t) + P_{NLOS,m}(t) \times PL_{NLOS,m}(t), \tag{5}$$

where $P_{LOS,m}$ and $P_{NLOS,m}$ are the LOS and NLOS probabilities of the aerial communication channel, respectively. The LOS probability can be expressed as [39]

$$P_{LOS,m,t} = \frac{1}{1 + a \cdot \exp(-b[\theta_{m,t} - a])}, \tag{6}$$

where a and b are constant values which depend on the environment and $\theta_{m,t}$ is the elevation angle in degrees. We can express $\theta_{m,t}$ as

$$\theta_{m,t} = \frac{180}{\pi} \times \sin^{-1}\left(\frac{h_U - h_m}{d_m(t)}\right). \tag{7}$$

Naturally, we have $P_{NLOS,m} = 1 - P_{LOS,m}$. The path loss for LOS and NLOS links between the UAV and the mth GBS is given by

$$\begin{aligned} PL_{LOS,m,t} &= d_m^{-\alpha_{LOS}}(t), \quad LOS\ link, \\ PL_{NLOS,m,t} &= d_m^{-\alpha_{NLOS}}(t), \quad NLOS\ link, \end{aligned} \tag{8}$$

where α_{LOS} and α_{NLOS} are the path loss exponents for the LOS and NLOS links, respectively. Note that we assume Rayleigh fading for both LOS and NLOS links [40].

C. DEFINITIONS OF PERFORMANCE METRICS

We are particularly interested in the optimal UAV trajectory with respect to the following performance metrics.

1) OUTAGE PROBABILITY

Outage probability defines the probability that the instantaneous received SNR of UAV is below a threshold. In principle, the distance between the UAV and the GBS affects the outage performance. At time t, the outage probability $P_{out}(t)$ of the terrestrial-aerial communication link is defined as

$$\begin{aligned} P_{out}(t) &= P(\gamma_t < \gamma_{th}) = P(\rho^2 < \frac{\gamma_{th}}{\lambda_t}) \\ &= \int_0^{\gamma_{th}} \frac{1}{\lambda_t} \cdot \exp(-\frac{x}{\lambda_t}) dx = 1 - \exp(-\frac{\gamma_{th}}{\lambda_t}), \end{aligned} \tag{9}$$

where γ_{th} is an SNR threshold. Also, we assume that the UAV is associated with the GBS based on the maximum received signal strength criterion, i.e., $\lambda_t = \gamma_0 \times \max_{m \in \mathbb{M}} PL_m(t)$. Based on this, the path loss depends on the distance between the UAV and the GBS. As a result, $P_{out}(t)$ varies with the UAV's locations. Here, we consider a communication link is reliable if its outage probability is smaller than a predefined value ε_{out}, i.e.,

$$P_{out}(t) \le \varepsilon_{out}. \tag{10}$$

Note that the value of ε_{out} can be determined by the desired quality of service.

2) CONNECTIVITY OUTAGE RATIO

A connectivity area A_c is defined as all the possible UAV points with reliable connectivity, i.e., u_t satisfies (10). Otherwise, u_t is in the outage area, denoted as A_o. Then, for a given trajectory P, we define the sets of points such that the UAV flies from A_c to A_o and from A_o to A_c as

$$\mathbb{Z} = \{u_t | u_t \in A_c, \lim_{\Delta \to 0} u_{t+\Delta} \in A_o, \quad t \in [0, T]\}, \tag{11}$$

$$\mathbb{Y} = \{u_t | u_t \in A_o, \lim_{\Delta \to 0} u_{t+\Delta} \in A_c, \quad t \in [0, T]\}. \tag{12}$$

Assume that u_0 and u_F are in the connectivity area A_c. We define the connectivity outage of P as the sum of subtrajectory length with points in the outage area, i.e.,

$$d_{P,out} = \sum_{y_i \in \mathbb{Y}, z_i \in \mathbb{Z}} \|y_i - z_i\|. \tag{13}$$

The total trajectory length can be calculated as

$$d_{P,total} = \sum_{i=1}^{S} \left\| u^i - u^{i-1} \right\|. \tag{14}$$

Then, the ratio of connectivity outage R_P can be expressed as

$$R_P = \frac{d_{P,out}}{d_{P,total}}. \tag{15}$$

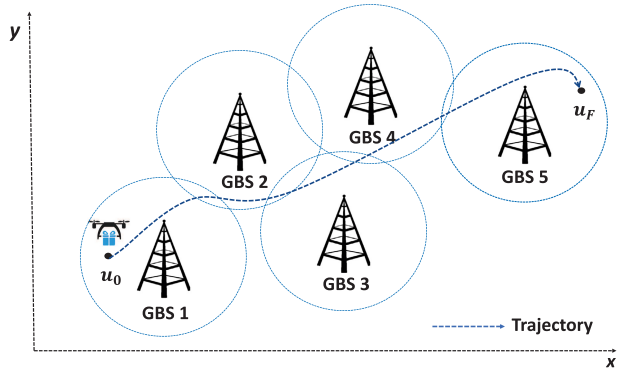

FIGURE 2. An illustration of trajectory design for a cellular-enabled UAV.

To satisfy the reliability requirement during the entire UAV mission, R_P should be guaranteed no larger than a given threshold R_{th}.

D. PROBLEM FORMULATION

Our objective in this paper is to minimize the mission completion time by optimizing the trajectory $P = \{u^s\}_{s\in\{0,\ldots,S\}}$. The optimization problem is formulated as follows

$$\min_{T,\ P=\{u^s\}} \quad T \tag{16a}$$
$$s.t.\ \ R_P \le R_{th} \tag{16b}$$
$$u(0) = u_0 \tag{16c}$$
$$u(T) = u_F \tag{16d}$$
$$h_U > h_m, m \in \mathbb{M} \tag{16e}$$
$$\frac{\|u(i) - u(j)\|}{i-j} \le V_{\max}, \quad 0 \le j < i \le T\,. \tag{16f}$$

The inequality constraint (16b) ensures that the ratio of connectivity outage R_P is no larger than a predefined threshold R_{th}. This constraint guarantees that the UAV maintains enough connectivity during the entire UAV mission. Furthermore, (16c) and (16d) guarantee that the UAV starts and ends at the requested locations. (16e) ensures that the UAV altitude is always higher than all the GBSs. (16f) guarantees the maximum UAV speed constraint. An example of the considered problem is shown in Fig. 2, where the connectivity areas covered by GBSs are represented by circles. In the next section, we will demonstrate the NP-hardness of problem (16).

IV. PROBLEM ANALYSIS

To solve the problem (16), we analyze the fundamentals based on graph transformation. Generally, the problem can be classified into two categories: (1) zero connectivity outage, i.e., UAV always connects with at least one GBS; (2) nonzero connectivity outage constraint, i.e., UAV is allowed to lose connectivity with the GBS in a tolerable time.

A. WITH ZERO CONNECTIVITY OUTAGE

In this case, we have $R_{th} = 0$ in the constraint (16b). We adopt a *graph* method proposed in [24] to show how to calculate the optimal trajectory using the shortest path algorithm. First,

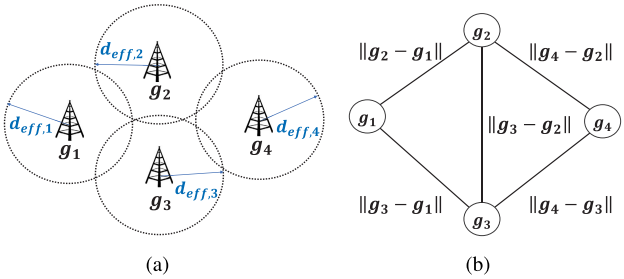

FIGURE 3. An illustration of transforming a GBS deployment into an undirected graph.

undirected weighted graph $G = (V, E)$ can be constructed, where V is given by

$$V = \{u_0, g_1, \ldots, g_M, u_F\}. \tag{17}$$

The coordinates of GBS, the start point, and the end point are modeled as vertices. To simplify the analysis, we assume that UAV flies at a fixed altitude $h_U > h_m$. Also, the edge set E is given by

$$\begin{aligned} E = &\{(u_0, g_m) : \|u_0 - g_m\| \le d_{eff,m},\ m \in M\} \\ &\cup \{(g_m, g_n) : \|g_m - g_n\| \le d_{eff,m} + d_{eff,n},\ m, n \in M,\ m \ne n\} \\ &\cup \{(u_F, g_m) : \|u_F - g_m\| \le d_{eff,m}, m \in M\}, \end{aligned} \tag{18}$$

where $d_{eff,m}$ is the maximum allowable distance of the mth GBS in order to satisfy the outage probability constraint (10). The weight of each edge is expressed as

$$\begin{aligned} W(u_0, g_m) &= \|u_0 - g_m\|, \\ W(g_m, g_n) &= \|g_m - g_n\|, \\ W(u_F, g_m) &= \|u_F - g_m\|, \quad m, n \in \mathbb{M},\ m \ne n. \end{aligned} \tag{19}$$

Note that $\|u_0 - g_m\| \le d_{eff,m}$ and $\|u_F - g_m\| \le d_{eff,m}$ mean that both the start and end points are in the connectivity area. Besides, $\|g_m - g_n\| \le 2d_{eff,m}$ means that the connectivity areas provided by the two GBSs are overlapped. To illustrate the graph construction, we give an example of four GBSs with different maximum allowable distances and its corresponding undirected graph as shown in Fig. 3(a) and Fig. 3(b), respectively.

Next, we derive the maximum allowable distance of GBSs.

Theorem 1: Let $\alpha_{LOS} = 2$ and $\alpha_{NLOS} = 4$. Given outage probability threshold ε_{out} and SNR threshold γ_{th}, $d_{eff,m}$ can be obtained as

$$\begin{aligned} d_{eff,m} &= \sqrt{\frac{P_{LOS,m} + \sqrt{P_{LOS,m}^2 + 4KP_{NLOS,m}}}{2K}}, \\ K &= \frac{\gamma_{th}}{\gamma_0 \times \ln(\frac{1}{1-\varepsilon_{out}})}. \end{aligned} \tag{20}$$

Proof: The maximum allowable distance of GBS can be found by solving the implicit equation

$$P_{out}(t) = \varepsilon_{out}. \tag{21}$$

From (9) and (10), we have

$$\varepsilon_{out} = 1 - \exp(-\frac{\gamma_{th}}{\lambda_t}). \quad (22)$$

It follows from (3) that we have

$$\exp(-\frac{\gamma_{th}}{\gamma_0 \times [P_{LOS,m} \times PL_{LOS,m} + P_{NLOS,m} \times PL_{NLOS,m}]}) = 1 - \varepsilon_{out}. \quad (23)$$

Replacing $PL_{LOS,m}$ and $PL_{NLOS,m}$ by (8), we are able to derive (20). The proof is completed. ■

By substituting (7) into (6), we have

$$P_{LOS,m,t} = \frac{1}{1 + a \cdot \exp(-b[\frac{180}{\pi} \times \sin^{-1}(\frac{h_{diff,m}}{d_m(t)}) - a])}, \quad (24)$$

where $h_{diff,m}$ is the different between h_U and h_m. We note that $P_{NLOS,m,t} = 1 - P_{LOS,m,t}$ with $P_{LOS,m,t}$ given in (6). From (20) and (24), we can observe the relation between the GBS coverage (i.e., maximum allowable distance) and the GBS height. Therefore, the UAV trajectory design should take both h_U and h_m into account, which will be shown through simulation in Section VI.

Based on the derived $d_{eff,m}$, the graph connectivity is obtained. Then, the UAV trajectory can be planned by finding the shortest path in graph G. Let the trajectory solved by the shortest path algorithm (e.g., Dijkstra) be denoted as $P_I = \{u_0, g_{I_1}, \ldots, g_{I_i}, \ldots, g_{I_N}, u_F\}, I_i \in \mathbb{M}$, where g_{I_i} is the coordinate of GBS along the path. Clearly, this trajectory is not the optimal solution as the UAV is required to fly above each GBS $g_{I_i}, i = 1, \ldots, N$.

An improved method based on intersection points is proposed in [24]. This method is called Q-method which is introduced below. Given two neighbor GBSs g_{I_n} and $g_{I_{n+1}}$, since the shape of each GBS connectivity area is a circle, there exists two intersection points on the boundary, given by $I_{n,n+1,1}$, $I_{n,n+1,2}$. Without loss of generality, we here assume the maximum allowable distance of the two neighbor GBSs are approximately equal, i.e., $d_{eff,n} \approx d_{eff,n+1}$. Then, we obtain a subtended angle $\theta_{I_n,I_{n+1}}$ formed by $I_{n,n+1,1}$, g_{I_n} and $I_{n,n+1,2}$, where $\theta_{I_n,I_{n+1}} \cong 2 \arccos(\frac{\|g_{I_n} - g_{I_{n+1}}\|}{d_{eff,n} + d_{eff,n+1}})$. Let $Q > 1$ denote the number of quantization level for dividing θ_{I_n,I_n+1} into $Q - 1$ equally spaced angle. We also define $u_{I_n,I_{n+1}}(q)$ as the qth point on the I_n connectivity boundary, where $q \in \mathbb{Q}, \mathbb{Q} = \{1, 2, \ldots, Q\}$. It can be expressed as

$$u_{I_n,I_{n+1}}(q) = d_{eff,I_n}[\cos\varphi, \sin\varphi]^T + g_{I_n},$$
$$\varphi = \phi_{I_n,I_{n+1}} + (\frac{q-1}{Q-1} - \frac{1}{2})\theta_{I_n,I_{n+1}}, \quad q \in \mathbb{Q}, \quad (25)$$

where $\phi_{I_n,I_{n+1}}$ denotes the angle between line $\overline{g_{I_n} g_{I_n+1}}$ and the x-axis. Intuitively, replacing the GBSs coordinates with these GBS connectivity boundary coordinates can help reduce the trajectory length since the UAV does not have to fly through every GBS on the path. Hence, the new graph $G_Q = (V_Q, E_Q)$ can be formulated by adding $u_{I_n,I_{n+1}}$ into (17). The vertex set V_Q and edge set E_Q are given as

$$V_Q = \{u_0, u_F\} \cup \{u_{m,n}(q) : \|g_m - g_n\| \le d_{eff,m} + d_{eff,n}, m, n \in \mathbb{M}, m \ne n, q \in \mathbb{Q}\}, \quad (26)$$

and

$$\begin{aligned} E_Q = &\{(u_0, u_{m,n}(q)) : \|u_0 - g_m\| \le d_{eff,m}, \\ &\quad m, n \in \mathbb{M}, m \ne n, \quad q \in \mathbb{Q}\} \\ &\cup \{(u_{m,n}(q), u_{n,l}(\hat{q})) : \|g_m - g_n\| \\ &\quad \le d_{eff,m} + d_{eff,n}, \|g_n - g_l\| \le d_{eff,m} + d_{eff,n}, \\ &\quad m, n, l \in \mathbb{M}, \ m \ne n, n \ne l, m \ne l, \quad q, \hat{q} \in \mathbb{Q}\} \\ &\cup \{(u_F, u_{m,n}(q)) : \|u_F - g_m\| \le d_{eff,m}, \\ &\quad m, n \in \mathbb{M}, \ m \ne n, \ q \in \mathbb{Q}\}. \end{aligned} \quad (27)$$

Similarly, the weight of each edge is given by

$$\begin{aligned} W_Q(u_0, u_{m,n}(q)) &: \left\|u_0 - u_{m,n}(q)\right\|, \\ W_Q(u_{m,n}(q), u_{n,l}(\hat{q})) &: \left\|u_{m,n}(q) - u_{n,l}(\hat{q})\right\|, \\ W_Q(u_{m,n}(q), u_F) &: \left\|u_{m,n}(q) - u_F\right\|, \quad m, n \in \mathbb{M}, \\ &\qquad m \ne n, q, \ \hat{q} \in \mathbb{Q}. \end{aligned} \quad (28)$$

The improved trajectory can be computed by applying the shortest path algorithm in graph G_Q. We note that a larger Q is more likely to obtain a shorter path as there are more diverse path candidates.

B. WITH NONZERO CONNECTIVITY OUTAGE CONSTRAINT

In this case, we consider that the UAV can fly to an outage area with a time period no larger than a non-zero threshold, i.e., $R_{th} > 0$ in the constraint (16b).

Theorem 2: For a given $R_{th} > 0$, the problem (16) is NP-hard.

Proof: See Appendix. ■

The work in [25] considered a similar problem but did not consider the effects of fading. A grid method based on dynamic programming was proposed in which an area is divided into N by M grid cells [41]. Then, dynamic programming is used to compute the optimal path within the entire grid. However, this method becomes infeasible when the area becomes large. To tackle this issue, we propose a graph based scheme to obtain the approximately optimal solution. This scheme is discussed in the next section.

V. PROPOSED TRAJECTORY DESIGN

In this section, we present our proposed intersection method based on enlarged coverage to solve problem (16). First, we improve the method proposed in [24] to design the UAV trajectory with zero connectivity outage constraint. Secondly, we investigate the optimal tradeoff between connectivity outage and trajectory length. To deal with the NP-hard problem with nonzero connectivity outage constraint, we propose the intersection method based on enlarged coverage to obtain the approximately optimal solution.

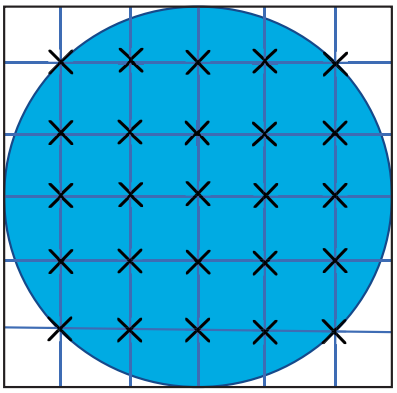

FIGURE 4. Illustration of the GBS coverage inscribed inside of a square where the sides of the square are tangent to the coverage circle. The square is divided into 6 × 6 sub-squares, resulting in 5 × 5 scattered points (indicated with ×).

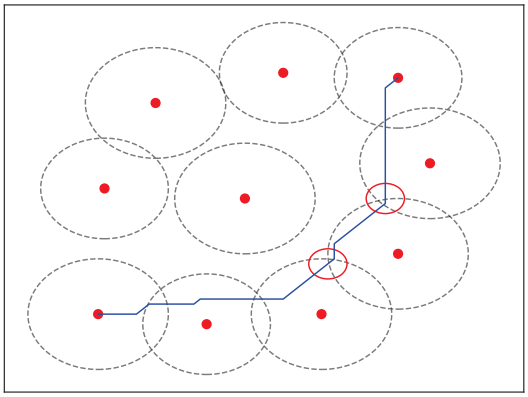

FIGURE 5. An example of a trajectory generated by the Dijkstra algorithm.

A. INTERSECTION METHOD

Consider a set of scattered points in the connectivity area of a GBS. Fig. 4 shows an example of 5 × 5 scattered points distributed in a square geometry. We assume that the UAV can only move between these scattered points. A trajectory can be formed by concatenating selected points with given start and end points. To avoid flying into the outage area, the UAV can only move to the nearest point in one of eight directions: north, north-east, east, south-east, south, south-west, west, and north-west. Then, we can use the shortest path algorithms to obtain the trajectory. Fig. 5 shows an example of a trajectory generated by the Dijkstra algorithm with dividing into 100 × 100 sub-squares in a GBS coverage. One can observe that this trajectory is not the shortest path. This is because the flight direction is limited. Moreover, we find that the intersection point (as indicated by the red circle) of two GBS coverage boundaries is the key to the design of optimal trajectory.

Next, we introduce our intersection method. We can calculate the intersection points between two neighbor GBSs for a given trajectory P_I. The set of intersection points can be defined as

$$\mathbb{U}=\{U_{1,2,1}, U_{1,2,2}, U_{2,3,1}, U_{2,3,2},\ldots, U_{N-1,N,1}, U_{N-1,N,2}\}, \tag{29}$$

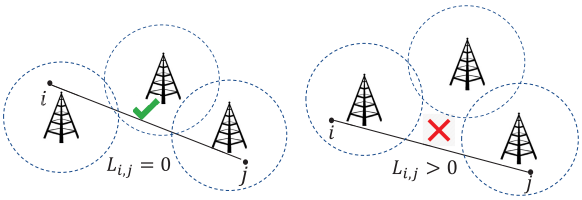

(a) Trajectory with $L_{i,j}=0$. (b) Trajectory with $L_{i,j}>0$.

FIGURE 6. Different cases of connectivity outage length $L_{i,j}$.

where $U_{n-1,n,1}$ and $U_{n-1,n,2}$ denote the intersection points between the coverage boundaries of $g_{I_{n-1}}$ and g_{I_n}. We have $U_{n-1,n,1} = U_{n-1,n,2}$ if there is only one intersection point between two neighbor GBSs. We define our graph $G_o=(V_o, E_o)$ based on intersection points. The set of vertex can be expressed as

$$V_o=\{u_0, u_F, \{U_{I_n,I_{n+1},1}, U_{I_n,I_{n+1},2}\}_{n=1}^{N-1}\}. \tag{30}$$

The principle of our intersection method is explained as follows. As illustrated in Fig. 6, two GBS connectivity area each exists two points i and j. We define connectivity outage length $L_{i,j}$ as the trajectory length within the outage area in which the UAV flies straight from i to j. In this case, we consider the UAV can fly from node i to j only if $L_{i,j}=0$. Therefore, the set of edge can be expressed as

$$\begin{aligned} E_o = &\{(U_{I_n,I_{n+1},w}, u_0) : L_{U_{I_n,I_{n+1},w},u_0}=0, w\in\{1,2\}\} \\ &\cup \{(U_{I_n,I_{n+1},w}, U_{I_m,I_{m+1},w}) : L_{U_{I_n,I_{n+1},w},U_{I_m,I_{m+1},w}}=0, \\ &\qquad w\in\{1,2\}\} \\ &\cup \{(U_{I_n,I_{n+1},w}, u_F) : L_{U_{I_n,I_{n+1},w},u_F}=0, w\in\{1,2\}\}. \end{aligned} \tag{31}$$

The weight of each edge is given by

$$\begin{aligned} W(U_{I_n,I_{n+1},w}, U_{I_m,I_{m+1},w}) &= \left\|U_{I_n,I_{n+1},w}-U_{I_m,I_{m+1},w}\right\|, \\ &\qquad w\in\{1,2\}, \\ W(U_{I_n,I_{n+1},w}, u_0) &= \left\|U_{I_n,I_{n+1},w}-u_0\right\|, \quad w\in\{1,2\}, \\ W(U_{I_n,I_{n+1},w}, u_F) &= \left\|U_{I_n,I_{n+1},w}-u_F\right\|, \quad w\in\{1,2\}. \end{aligned} \tag{32}$$

Based on the graph G_o, we can use the Dijkstra algorithm to find the shortest trajectory P_o.

Next, we analyze the effectiveness of our proposed intersection method. First, we show that our method can find a trajectory with a small number of turning points where the UAV has to change its direction. Clearly, a path with more turning points tends to have a longer length. Hence, the shortest path algorithm will ignore paths with many turning points and will choose those paths with least turning points. Secondly, we show that each subtrajectory generated in our method is the shortest. Consider a subtrajectory connected by three turning points. As shown in Fig. 7, assume that the UAV flies from point A to point C. Using our intersection method, the output trajectory will be $\{A, U_{a,b,2}, U_{b,c,2}, C\}$. In Fig. 8, consider triangle S_l formed by A, $U_{a,b,2}$, and $U_{b,c,2}$. Extending $\overline{AU_{a,b,2}}$ and $\overline{U_{a,b,2}U_{b,c,2}}$ to any boundary that is

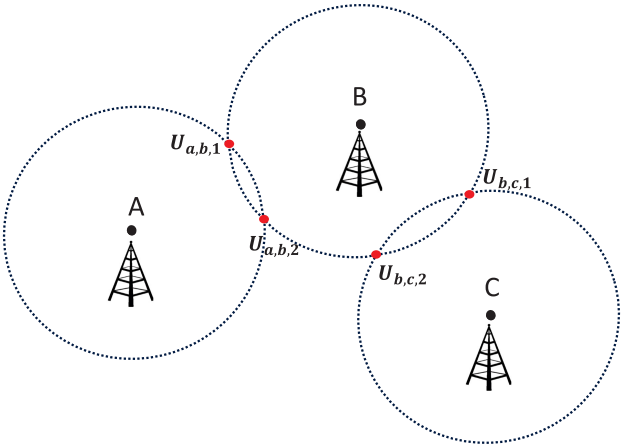

FIGURE 7. An example of the three-GBS scenario where the UAV flies from point A to point C.

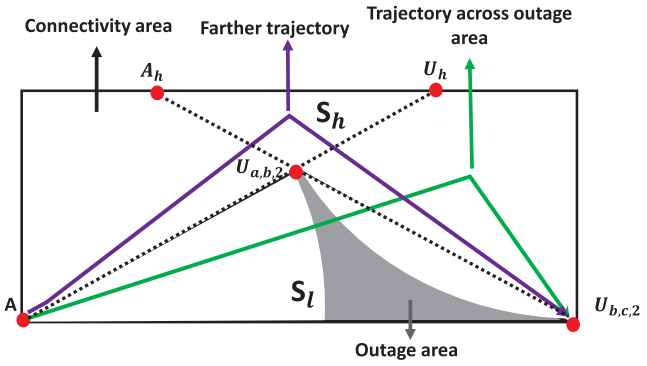

FIGURE 8. Analysis of subtrajectory with intersection points and outage area.

parallel to $\overline{AU_{b,c,2}}$ in connectivity area, we can obtain point A_h and U_h and a triangle S_h formed by $U_{a,b,2}$, A_h, and U_h. To find another subtrajectory shorter than $\{A, U_{a,b,2}, U_{b,c,2}\}$, we need to replace $U_{a,b,2}$ in subtrajectory $\{A, U_{a,b,2}, U_{b,c,2}\}$. For example, we can choose a point which is closer to $U_{b,c,2}$ to replace $U_{a,b,2}$. The resulting new subtrajectory is illustrated as the green line in the figure. However, this subtrajectory passes through the outage area. In fact, any point that is not in the triangle S_h will yield a subtrajectory that passes through the outage area. On the other hand, the new subtrajectory will be longer than $\{A, U_{a,b,2}, U_{b,c,2}\}$ if we replace $U_{a,b,2}$ with a point that is in the triangle S_h. The same property exists for $\{U_{a,b,2}, U_{b,c,2}, C\}$. Therefore, our method can find the shortest path in case of zero connectivity outage.

B. INTERSECTION METHOD BASED ON ENLARGED COVERAGE

We extend the intersection method to the problem with nonzero connectivity outage constraint. First, we analyze the tradeoff between connectivity outage ratio and trajectory length in a simplified case. As shown in Fig. 9, consider an area consisting of three GBSs located at points A, B, and C. Each GBS has connectivity area of radius r_A, r_B, r_C, respectively. Let $\overline{AB} = \alpha$, $\overline{BC} = \beta$, and $\overline{AC} = \gamma$.

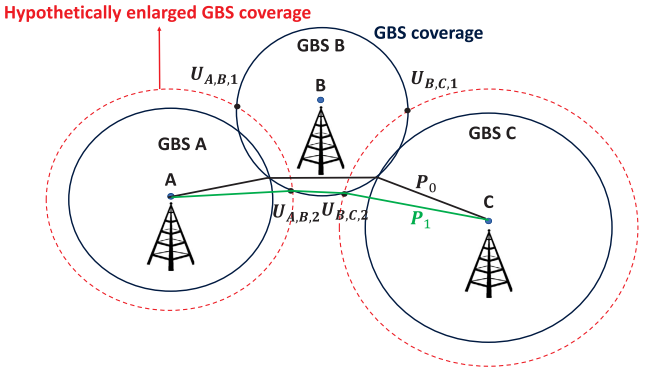

FIGURE 9. An example of the three-GBS scenario with enlarged coverage.

By using the above mentioned intersection method, we can find trajectory P_0. However, there exists a shorter trajectory if the trajectory is allowed to pass through the outage area. To show this, we hypothetically enlarge r_A and r_C. By using the intersection method, we can obtain another trajectory P_1 which is shorter than P_0.

With the enlarged coverage, the maximum allowable distance of GBS is given by

$$d_{eff,m,\varepsilon} = d_{eff,m} + 10\varepsilon, \quad m \in \mathbb{M}, \quad \varepsilon \in R^+, \tag{33}$$

where ε is the enlarged coefficient. Consider the three-GBS scenario with enlarged connectivity area as shown in Fig. 9. $U_{A,B,1}$ and $U_{A,B,2}$ are the intersection points between GBS A and GBS B. Also, $U_{B,C,1}$ and $U_{B,C,2}$ are the intersection points between GBS B and GBS C. The trajectory of enlarged method is $\{A, U_{A,B,2}, U_{A,B,2}, C\}$ as green line in Fig. 9. The subtrajectory length of $\overline{AU_{A,B,2}}$ and $\overline{U_{B,C,2}C}$ are $r_A + 10\varepsilon$ and $r_C + 10\varepsilon$, respectively. To calculate the trajectory length $\overline{U_{A,B,2}U_{B,C,2}}$, we define the following angles: $\tau \triangleq \angle AU_{A,B,2}B$, $\upsilon \triangleq \angle BU_{B,C,2}C$, and $\omega \triangleq \angle ABC$. Using the law of cosine, we have

$$\begin{aligned}
\tau &= \cos^{-1}\left(\frac{(r_A + 10\varepsilon)^2 + r_B^2 - \alpha^2}{2(r_A + 10\varepsilon)r_B}\right), \\
\upsilon &= \cos^{-1}\left(\frac{(r_C + 10\varepsilon)^2 + r_B^2 - \beta^2}{2(r_C + 10\varepsilon)r_B}\right), \\
\omega &= \cos^{-1}\left(\frac{\alpha^2 + \beta^2 - \gamma^2}{2\alpha\beta}\right).
\end{aligned} \tag{34}$$

Since quadrilaterals $A{-}U_{A,B,1}{-}B{-}U_{A,B,2}$ and $B{-}U_{B,C,1}{-}C{-}U_{B,C,2}$ are diamond shapes, we can define the following angles:

$$\begin{aligned}
\xi &\triangleq \angle U_{A,B,1}BU_{A,B,2} = 180^\circ - \tau, \\
\psi &\triangleq \angle U_{B,C,1}BU_{B,C,2} = 180^\circ - \upsilon, \\
\varpi &\triangleq \angle U_{A,B,2}BU_{B,C,2} = \omega - 0.5(\xi + \psi).
\end{aligned} \tag{35}$$

Then, we have

$$\overline{U_{A,B,2}U_{B,C,2}} = \sqrt{2r_B^2 - 2r_B^2\cos(\varpi)}. \tag{36}$$

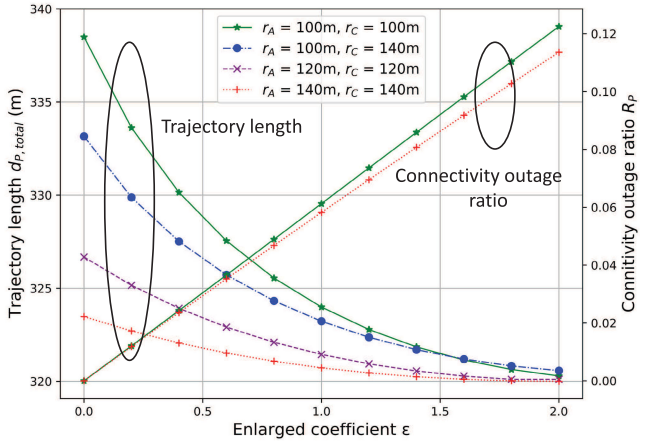

FIGURE 10. The trend chart of connectivity outage ratio R_P and trajectory length $d_{P,total}$ for different coverage radius of GBS A and GBS C.

The total trajectory length $d_{P_\varepsilon,total}$ and the connectivity outage length $d_{P_\varepsilon,out}$ can be expressed as

$$\begin{aligned} d_{P_\varepsilon,total} &= \sqrt{2r_B^2 - 2r_B^2\cos(\varpi)} + r_A + r_C + 20\varepsilon, \\ d_{P_\varepsilon,out} &= 20\varepsilon. \end{aligned} \tag{37}$$

Based on (15) and (16b), the following inequality holds for any given R_{th}

$$R_P = \frac{20\varepsilon}{\sqrt{2r_B^2 - 2r_B^2\cos(\varpi)} + r_A + r_C + 20\varepsilon} \leq R_{th}. \tag{38}$$

From Fig. 10, we can observe the tradoff between the connectivity outage ratio and trajectory length. It is reasonable that the trajectory length decreases as the coverage range increases. This is because the increase of coverage range leads to more feasible subtrajectories. With the increase of ε, the gap of trajectory length for different coverage radius becomes smaller since the GBS with small coverage radius can find a shorter trajectory. On the other hand, if the initial connectivity area is large, the gain of hypothetically enlarging GBS coverage area is limited. Moreover, the connectivity outage ratio becomes large as ε increases due to the increased possibility of flying into the outage area.

Then, we have the following theorem regarding the proposed method.

Theorem 3: Our proposed intersection method based on enlarged coverage can achieve the optimal tradeoff in the three-GBS scenario as shown in Fig. 8.

Proof: In Section V, we have proved that using intersection method can find the shortest trajectory in case of having zero connectivity outage constraint. For the case of having nonzero connectivity outage constraint, we adopt enlarged coverage to obtain a more connected graph. Such a new graph can be considered as having zero connectivity outage constraint with larger GBS coverage area. Note that the connectivity outage ratio will increase as the enlarged coefficient increases. Hence, by gradually increasing the enlarged coefficient, the optimal tradeoff such that $R_P = R_{th}$ can be obtained. ■

Although we can find the optimal tradeoff solution in the simplified case, problem (16) is still an NP-hard problem in general. To this end, we propose a polynomial time algorithm to approximate the optimal trajectory. The proposed algorithm is presented in Algorithm 1.

Algorithm 1 Intersection Method Based on Enlarged Coverage Algorithm

Input: $u_0, u_F, \{g_m\}_{m=1}^M, \{d_{eff,m,\varepsilon}\}_{m=1}^M, R_{th}$
Output: P_{opt}

$\varepsilon = 0$
while $(R_{P_{opt}} \leq R_{th})$ **do**
  Construct an undirected weighted graph $G_\varepsilon = (V_\varepsilon, E_\varepsilon)$ according to (17), (18) and (19).
  Obtain the shortest path from u_0 to u_F in G_ε via Dijkstra algorithm. Denote the selected GBSs as $\mathbb{I}_\varepsilon = [g_{I_{1,\varepsilon}}, g_{I_{2,\varepsilon}}, \ldots, g_{I_{i,\varepsilon}}, \ldots, g_{I_{N,\varepsilon}}], I_{i,\varepsilon} \in \mathbb{M}$.
  Utilize the selected GBSs set $\mathbb{I}_\varepsilon$ to construct an undirected weighted graph $G_{o,\varepsilon} = (V_{o,\varepsilon}, E_{o,\varepsilon})$ according to (30), (31), and (32).
  Obtain the shortest path from u_0 to u_F in $G_{o,\varepsilon}$ via Dijkstra algorithm. Denote the trajectory and the ratio of outage connectivity as P_ε and R_ε, respectively.
  $P_{opt} \leftarrow P_\varepsilon$
  $R_{P_{opt}} \leftarrow R_\varepsilon$
  $\varepsilon \leftarrow \varepsilon + 1$
  if $R_{P_{opt}} > R_{th}$ **then**
    $P_{opt} \leftarrow P_{\varepsilon-1}$
  end if
end while

Given outage connectivity ratio threshold R_{th} and GBS coordinates, our algorithm can obtain an approximate optimal trajectory P_{opt}. First, we set $\varepsilon = 0$ and construct a graph G_ε with the maximum allowable distance $d_{eff,m,\varepsilon}$ based on (20). Then, by using Dijkstra algorithm, we can find a trajectory in which the UAV passes through all the coordinates of a GBS set, denoted by $\mathbb{I}_\varepsilon$. After that, we construct a graph $G_{o,\varepsilon}$ by calculating the intersection points in set $\mathbb{I}_\varepsilon$ to obtain the shortest trajectory P_{opt} in $G_{o,\varepsilon}$. From (15), we can calculate the connectivity outage ratio $R_{P_{opt}}$. After each iteration, if $R_\varepsilon \leq R_{TH}$, the value of enlarged coefficient ε will be increased. As ε increases, the maximum allowable distance increases, i.e, $d_{eff} < d'_{eff}$. Therefore, by increasing ε, we can obtain a shorter trajectory but with a larger connectivity outage ratio, i.e., $d_{total} > d'_{total}$ and $R < R'$. A graphical illustration of the relation is shown in Fig. 11. Finally, we can find an approximate shortest trajectory.

Now, we compare our method against state-of-the-art trajectory design methods proposed in [24] and [25]. The authors of [24] solve the problem in the case of zero connectivity outage constraint by using Dijkstra algorithm, which has time complexity $O(M^4Q^2)$, where M is the number of GBSs and Q is the number of additional vertices added to the graph. The authors of [25] consider the problem in the case

TABLE 2. Comparison of the proposed method with [24] and [25].

Problem	Problem Reformulation	Method	Time Complexity
Trajectory optimization problem [24]	Shortest path	Dijkstra with Q-method	$O(M^4Q^2)$
Trajectory optimization problem with connectivity constraint [25]	Shortest path in grid-based area	Dynamic programming	$O(XWL)$
Trajectory optimization problem with connectivity outage constraint	Shortest path with removable obstacle	Dijkstra with intersection method based on enlarged coverage	$O(M^4N)$

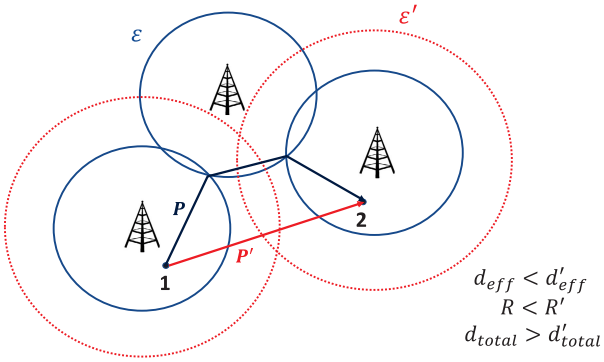

FIGURE 11. Illustration of the UAV trajectory obtained with different enlarged coefficient ε.

of nonzero connectivity outage constraint and reformulate the problem by dividing the flight area into $W \times L$ grid (in meters). A dynamic programming algorithm is proposed, which has time complexity $O(XWL)$, where X is a parameter for flight direction control. However, such grid-based method is not feasible in wide-area environments. On the other hand, the complexity of our proposed algorithm has two main contributors, namely the enlarged coefficient search and the Dijkstra algorithm. The proposed scheme involves two shortest path computation using Dijkstra algorithm during each iteration of the enlarged coefficient search. The first shortest path computation obtains an initial trajectory, which requires $O(M^2)$ comparisons [42]. In the second shortest path computation, all the intersection points are included in the graph, resulting in $2 + 2M(M-1)$ vertices in the worst case. Therefore, the total computational complexity of the proposed algorithm is $O(((M+2)^2+(2+2M(M-1))^2)N) \approx O(M^4N)$, where N is the number of iterations conducted for searching ε. In case of zero connectivity outage constraint (i.e., $\varepsilon = 0$), we have $N = 1$. Therefore, the complexity of our algorithm is $O(M^4)$, which is less than Q-method [24].

VI. NUMERICAL RESULTS

A. SIMULATION SETUP

To evaluate the performance of the proposed method, we perform simulations for both cases with zero and nonzero connectivity outage constraints. In principle, our method can be applied to any type of UAV. To better highlight the simulations, the system parameters are selected based on the properties of rotary-wing UAV [43], which is popular in package delivery and sensing applications. The limited flight time of the rotary-wing UAV is up to an hour, and the maximum speed is 30 m/s [44], [45]. In addition, the flight altitude is limited to less than 130 m required by the existing UAV regulations [43].

TABLE 3. Simulation parameters.

Notations	Parameter	Setting
M	Number of GBSs	24
h_U	UAV altitude	100 m, 120 m
u_0, u_F	Start and end position	$(100, 100, h_U), (850, 970, h_U)$
γ_{th}	SNR threshold	5 dB
ε_{out}	Outage probability threshold	0.1
h_m	GBS height	20 m, uniformly distributed over [20,40] m
$V_{\max}$	Maximum UAV speed	20 m/s

We assume that UAV flies within an area of size 1 km $\times$ 1 km, containing 24 GBSs. For the UAV channel model, we follow the urban macro (UMa) scenario suggested by the 3GPP [3]. For the case of zero connectivity outage constraint, we compare the performance of Q-method [24] in terms of trajectory length. In order to do a fair comparison, we assume that all the GBS have an equal size of connectivity area as in [24]. Note that we do not compare against the method described in [25] as it cannot scale to wide-area environments. In the case of having nonzero connectivity outage constraint, we further consider GBS with different sizes of connectivity area. Other simulation parameters are given in Table. 3.

B. PERFORMANCE COMPARISON

First, we compare the results in case of having zero connectivity outage constraint. Fig. 12 shows the UAV flight trajectory under two different GBS deployment scenarios. In this case, we set Q = 2 for Q-method and $\varepsilon = 0$ for the proposed method. For both GBS deployments, we can observe that our method can obtain a shorter trajectory with less complexity compared to Q-method. This is because that our method can avoid the unnecessary path segments containing intersection points.

In Fig. 13, we compare the trajectory length performances of different methods with $\varepsilon_{out} = 0.13$. Compared with Fig. 12, we can observe that the trajectory length becomes shorter as ε_{out} grows. This is because that the maximum allowable distance increases when ε_{out} increases. Also, it is shown that the proposed method can find a shorter trajectory, regardless the value of ε_{out}.

Here we show the results in case of having nonzero connectivity outage constraint. We assume that GBSs have different sizes of connectivity area and their altitudes are assumed

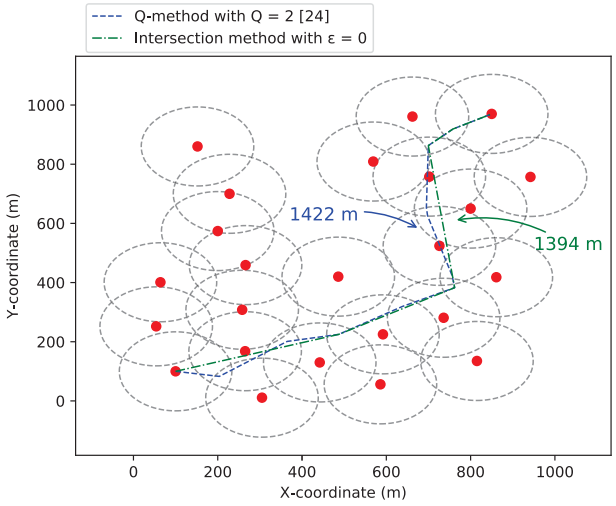

(a) GBS scenario 1.

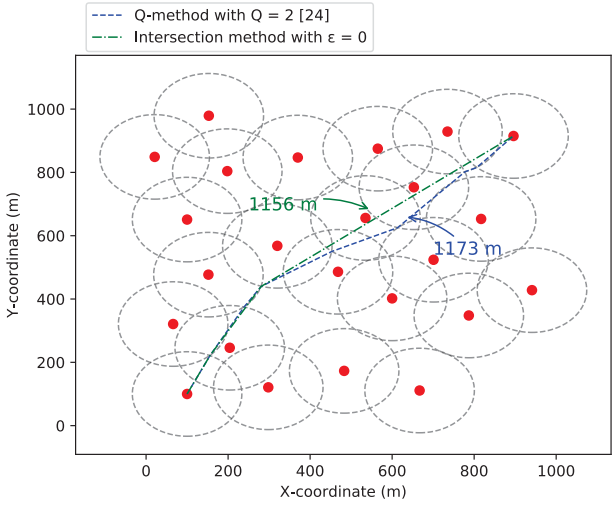

(b) GBS scenario 2.

FIGURE 12. Trajectory length comparisons for different trajectory design methods with $h_U = 120$ m and $\varepsilon_{out} = 0.1$.

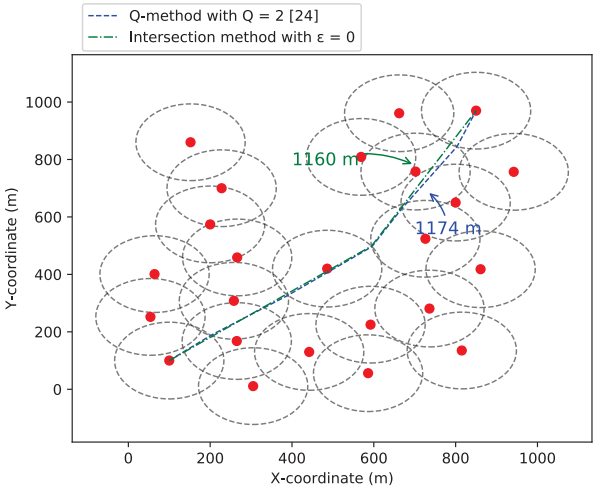

FIGURE 13. Trajectory length comparisons for different trajectory design methods with $h_U = 120$ m and $\varepsilon_{out} = 0.13$.

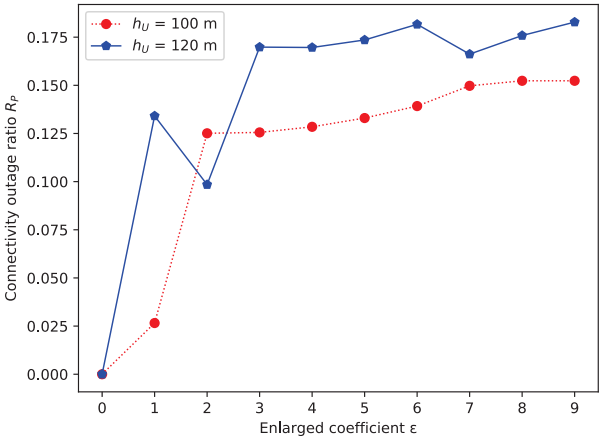

FIGURE 14. Connectivity outage ratio vs. enlarged coefficient with $h_U = 100, 120$ m.

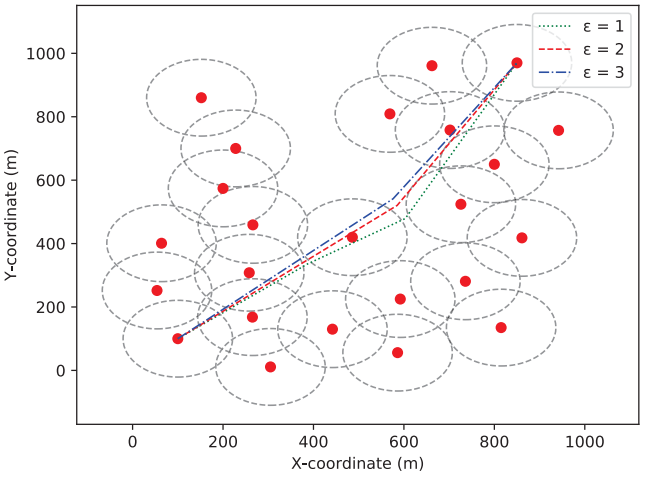

FIGURE 15. Trajectory with respect to enlarged coefficient ε with $h_U = 100$ m.

to follow the uniform distribution, i.e., $h_m \in U[20, 40]$. As shown in Fig. 14, the connectivity outage ratio increases as the enlarged coefficient increases. It is observed that the outage ratio with $h_U = 100$ m is less than that with $h_U = 120$ m. One reason for this is because the higher altitude of UAVs leads to a higher path loss. Note that it is reduced to the case of having zero connectivity outage constraint if $\varepsilon = 0$.

In Figs. 15 and 16, we compare the UAV trajectory with different enlarged coefficients under $h_U = 100$ m and 120 m, respectively. It shows that enlarging coverage area can shorten the trajectory, but paying the cost of increasing outage connectivity ratio. From Fig. 15, we can observe that the trajectory length is decreased smoothly as ε increases. When $h_U = 120$ m, we observe that the trajectories length drops significantly for $\varepsilon = 1, 2, 3$. It shows that the trajectory length can be significantly shortened if ε is increased. Besides, the trajectory length becomes shorter as the h_U decreases from 120 m to 100 m. These results show how different altitudes affect the optimal decision of the

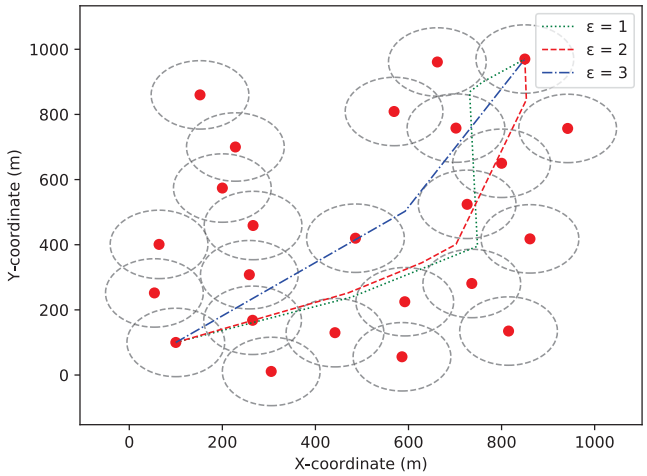

FIGURE 16. Trajectory with respect to enlarged coefficient ε with $h_U = 120$ m.

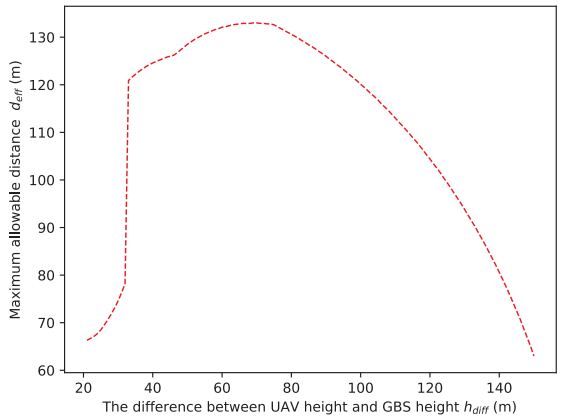

FIGURE 17. The relationship between h_{diff} and the maximum allowable distance d_{eff}.

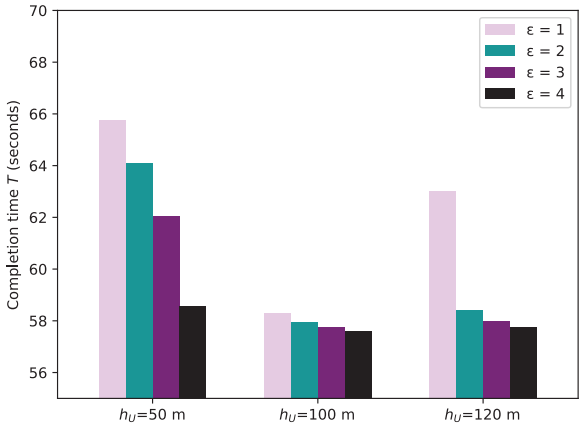

(a) Completion time performances.

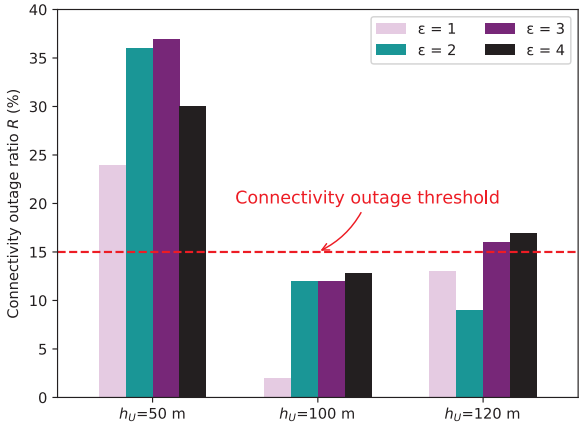

(b) Connectivity outage performances.

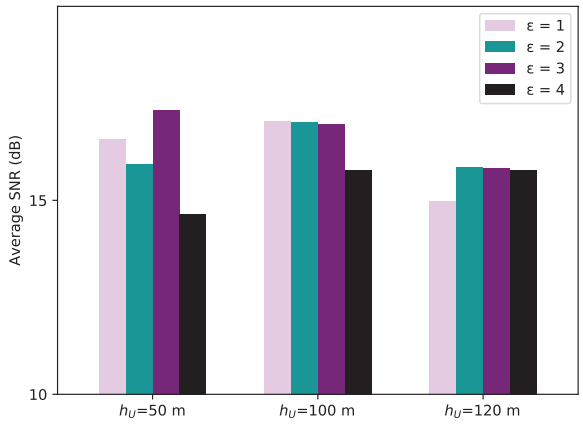

(c) Average SNR performances.

FIGURE 18. Performance results of the proposed method with $h_U = 50$, 100, and 120 m.

enlarged coefficient. For the aerial communication channel, a high altitude leads to a high LOS probability but at the cost of higher path loss [46]. Hence, the connectivity area is related to the altitude of UAV. We also show the relationship between h_{diff} and the GBS coverage in Fig. 17. We can observe that the maximum allowable distance is achieved when h_{diff} is around 70 m. These results can help a system designer fine tune parameters such as UAV altitude h_U and enlarged coefficient ε to obtain the shortest trajectory.

Figure 18 characterizes the performance of the proposed trajectory design method in terms of completion time, connectivity outage ratio, and average SNR over the entire flight duration. The connectivity outage ratio threshold is considered equal to 0.15 in our simulations. It is observed that the connectivity outage requirement can be achieved by adjusting the UAV altitude or enlarged coefficient. When $h_U = 120$ m, only $\varepsilon = 1, 2$ can satisfy the connectivity outage requirement. In comparison, $\varepsilon = 1, 2, 3, 4$ can satisfy the connectivity outage requirement when $h_U = 100$ m. However, all $\varepsilon = 1, 2, 3, 4$ cannot satisfy the connectivity outage requirement when $h_U = 50$ m. Also, the UAV altitude and enlarged coefficient can be jointly designed to achieve the optimal performance. In this case, $h_U = 100$ m and $\varepsilon = 4$ outperforms all the other combinations in terms of completion time under the connectivity outage requirement. Besides, we observe that the average SNR will not be affected by the increase of enlarged coefficient. The reason is that our method

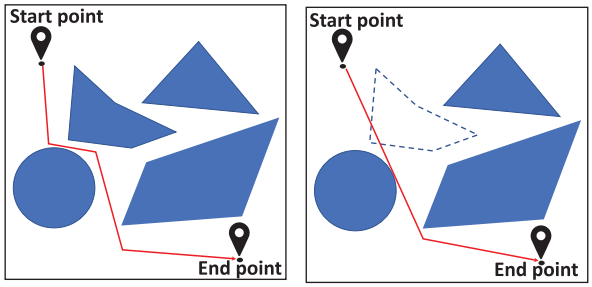

(a) A trajectory in the presence of obstacles. (b) A shorter trajectory with an obstacle being removed.

FIGURE 19. Illustration of the obstacle-removing shortest path problem.

can limit the maximum distance between the UAV and GBS, as we can see from Figs. 15 and 16. This shows that our method is robust and the average performance is not sensitive to the exact choice of ε.

VII. CONCLUSION

This paper studied the trajectory design problem in a cellular-enabled UAV system for maintaining reliable wireless connectivity with the ground base stations (GBSs). We have proposed a novel formulation of the trajectory optimization problem in which the connectivity outage ratio of the trajectory is constrained to be no larger than a predefined threshold. We have proved the formulated problem is NP-hard and revealed a tradeoff between trajectory length and connectivity outage ratio by using graph theory. By exploiting the observed structure, a low-complexity method was proposed to obtain an approximate optimal solution. Our numerical results validated the efficacy of the proposed method. In future work, the optimal techniques for 3D UAV trajectory design considering the inter-cell interference will be studied.

APPENDIX

In order to prove that problem (16) is NP-hard, we first introduce a known NP-hard decision problem: obstacle-removing shortest path problem (ORSPP) [47]. This problem generalizes a natural formulation in robot planning settings. In many robot applications, removing a few blockages during operation can greatly shorten the travel path. Hence, the model of ORSPP is useful in which a robot can adapt the environment to enable a better path.

In ORSPP, given a start point s at (x_1, y_1) and an end point t at (x_2, y_2), the objective of a path planner is to find the shortest path $s - t$ in an environment with several removable obstacles. In particular, the path planner can make the path shorter by paying cost to remove some obstacles as illustrated in Fig. 19(a). Formally, an ORSPP is defined as follows. Let $K = \{k_1, k_2, \ldots, k_n\}$ be a set of n removable obstacles. Each obstacle k_i can be removed by paying cost c_i for $i = 1, 2, \ldots, n$. We want to find the shortest path $s - t$ whose cost is at most a given budget B.

Next, we show that ORSPP can be reduced to problem (16) within polynomial steps. Without loss of generality, we consider the 2D trajectory design in which the UAV flies at a constant altitude. The connectivity area can be considered as the feasible area, while the outage area can be viewed as the area with obstacles as shown in Fig. 19(a). For a given trajectory P, we define the cost c_i as the subtrajectory length with points in the outage area, i.e.,

$$c_i = \|y_i - z_i\|, \tag{39}$$

where $y_i \in \mathbb{Y}$ and $z_i \in \mathbb{Z}$ are defined as (11) and (12). Since y_i and z_i are fixed depending on the locations and the coverage radius of all the GBSs, we can decide appropriate c_i for a given GBS deployment scenario. Then, the cost budget can be transformed to the constraint of the trajectory length within the outage area, i.e.,

$$B = R_{th} \times d_{P,total}. \tag{40}$$

In this way, we have transformed ORSPP to problem (16). Given that ORSPP is NP-hard, problem (16) must also be NP-hard.

REFERENCES

[1] S. Hayat, E. Yanmaz, and R. Muzaffar, "Survey on unmanned aerial vehicle networks for civil applications: A communications viewpoint," *IEEE Commun. Surveys Tuts.*, vol. 18, no. 4, pp. 2624–2661, 4th Quart., 2016.

[2] C. Zhan, Y. Zeng, and R. Zhang, "Energy-efficient data collection in UAV enabled wireless sensor network," *IEEE Wireless Commun. Lett.*, vol. 7, no. 3, pp. 328–331, Jun. 2018.

[3] *Study on Enhanced LTE Support for Aerial Vehicles (Release 15)*, document TR 36.777, 3GPP, Dec. 2017. [Online]. Available: http://www.3gpp.org/ftp//Specs/archive/36_series/36.777/

[4] Y. Zeng, J. Lyu, and R. Zhang, "Cellular-connected UAV: Potential, challenges, and promising technologies," *IEEE Wireless Commun.*, vol. 26, no. 1, pp. 120–127, Feb. 2019.

[5] *Study on Remote Identification of Unmanned Aerial Systems (Release 16)*, document TR 22.825, 3GPP, Sep. 2018. [Online]. Available: https://www.3gpp.org/ftp/Specs/archive/22_series/22.825/

[6] X. Yuan, Z. Feng, W. Xu, W. Ni, J. A. Zhang, Z. Wei, and R. P. Liu, "Capacity analysis of UAV communications: Cases of random trajectories," *IEEE Trans. Veh. Technol.*, vol. 67, no. 8, pp. 7564–7576, Aug. 2018.

[7] S. Wu, R. Atat, N. Mastronarde, and L. Liu, "Improving the coverage and spectral efficiency of millimeter-wave cellular networks using device-to-device relays," *IEEE Trans. Commun.*, vol. 66, no. 5, pp. 2251–2265, May 2018.

[8] Y. Yang, Z. Hu, K. Bian, and L. Song, "ImgSensingNet: UAV vision guided aerial-ground air quality sensing system," in *Proc. IEEE Conf. Comput. Commun.*, Apr. 2019, pp. 1207–1215.

[9] Q. Wu, Y. Zeng, and R. Zhang, "Joint trajectory and communication design for multi-UAV enabled wireless networks," *IEEE Trans. Wireless Commun.*, vol. 17, no. 3, pp. 2109–2121, Mar. 2018.

[10] Z. M. Fadlullah, D. Takaishi, H. Nishiyama, N. Kato, and R. Miura, "A dynamic trajectory control algorithm for improving the communication throughput and delay in UAV-aided networks," *IEEE Netw.*, vol. 30, no. 1, pp. 100–105, Jan. 2016.

[11] Y. Zeng, R. Zhang, and T. J. Lim, "Throughput maximization for UAV-enabled mobile relaying systems," *IEEE Trans. Commun.*, vol. 64, no. 12, pp. 4983–4996, Dec. 2016.

[12] M. Hua, L. Yang, C. Pan, and A. Nallanathan, "Throughput maximization for full-duplex UAV aided small cell wireless systems," 2019, *arXiv:1912.04532*. [Online]. Available: https://arxiv.org/abs/1912.04532

[13] H. Kang, J. Joung, J. Ahn, and J. Kang, "Secrecy-aware altitude optimization for quasi-static UAV base station without eavesdropper location information," *IEEE Commun. Lett.*, vol. 23, no. 5, pp. 851–854, May 2019.

[14] Y. Pan, S. Li, J. L. Chang, Y. Yan, S. Xu, Y. An, and T. Zhu, "An unmanned aerial vehicle navigation mechanism with preserving privacy," in *Proc. IEEE Int. Conf. Commun. (ICC)*, May 2019, pp. 1–6.

[15] X. Zhou, S. Yan, J. Hu, J. Sun, J. Li, and F. Shu, "Joint optimization of a UAV's trajectory and transmit power for covert communications," *IEEE Trans. Signal Process.*, vol. 67, no. 16, pp. 4276–4290, Aug. 2019.
[16] Y.-J. Chen and L.-C. Wang, "Privacy protection for Internet of drones: A network coding approach," *IEEE Internet Things J.*, vol. 6, no. 2, pp. 1719–1730, Apr. 2019.
[17] X. C. Chen and Y. J. Chen, "A machine learning based attack in UAV communication networks," in *Proc. IEEE 90th Veh. Technol. Conf.*, Sep. 2019, pp. 1–2.
[18] M. Hua, Y. Wang, Q. Wu, H. Dai, Y. Huang, and L. Yang, "Energy-efficient cooperative secure transmission in multi-UAV-enabled wireless networks," *IEEE Trans. Veh. Technol.*, vol. 68, no. 8, pp. 7761–7775, Aug. 2019.
[19] X. Cao, J. Xu, and R. Zhangt, "Mobile edge computing for cellular-connected UAV: Computation offloading and trajectory optimization," in *Proc. IEEE 19th Int. Workshop Signal Process. Adv. Wireless Commun. (SPAWC)*, Jun. 2018, pp. 1–5.
[20] S. Jeong, O. Simeone, and J. Kang, "Mobile edge computing via a UAV-mounted cloudlet: Optimization of bit allocation and path planning," *IEEE Trans. Veh. Technol.*, vol. 67, no. 3, pp. 2049–2063, Mar. 2018.
[21] Y. Qian, F. Wang, J. Li, L. Shi, K. Cai, and F. Shu, "User association and path planning for UAV-aided mobile edge computing with energy restriction," *IEEE Wireless Commun. Lett.*, vol. 8, no. 5, pp. 1312–1315, Oct. 2019.
[22] M. A. Abd-Elmagid and H. S. Dhillon, "Average peak age-of-information minimization in UAV-assisted IoT networks," *IEEE Trans. Veh. Technol.*, vol. 68, no. 2, pp. 2003–2008, Feb. 2019.
[23] C. Zhou, H. He, P. Yang, F. Lyu, W. Wu, N. Cheng, and X. Shen, "Deep RL-based trajectory planning for AoI minimization in UAV-assisted IoT," in *Proc. 11th Int. Conf. Wireless Commun. Signal Process. (WCSP)*, Oct. 2019, pp. 1–6.
[24] S. Zhang, Y. Zeng, and R. Zhang, "Cellular-enabled UAV communication: A connectivity-constrained trajectory optimization perspective," *IEEE Trans. Commun.*, vol. 67, no. 3, pp. 2580–2604, Mar. 2019.
[25] E. Bulut and I. Guevenc, "Trajectory optimization for cellular-connected UAVs with disconnectivity constraint," in *Proc. IEEE Int. Conf. Commun. Workshops (ICC Workshops)*, May 2018, pp. 1–6.
[26] Y. Zeng, X. Xu, and R. Zhang, "Trajectory design for completion time minimization in UAV-enabled multicasting," *IEEE Trans. Wireless Commun.*, vol. 17, no. 4, pp. 2233–2246, Apr. 2018.
[27] C. You and R. Zhang, "3D trajectory optimization in Rician fading for UAV-enabled data harvesting," *IEEE Trans. Wireless Commun.*, vol. 18, no. 6, pp. 3192–3207, Jun. 2019.
[28] Q. Wu, L. Liu, and R. Zhang, "Fundamental trade-offs in communication and trajectory design for UAV-enabled wireless network," *IEEE Wireless Commun.*, vol. 26, no. 1, pp. 36–44, Feb. 2019.
[29] X. Liu, M. Chen, and C. Yin, "Optimized trajectory design in UAV based cellular networks: A double Q-learning approach," in *Proc. IEEE Int. Conf. Commun. Syst. (ICCS)*, Dec. 2018, pp. 13–18.
[30] H. Bayerlein, P. De Kerret, and D. Gesbert, "Trajectory optimization for autonomous flying base station via reinforcement learning," in *Proc. IEEE 19th Int. Workshop Signal Process. Adv. Wireless Commun. (SPAWC)*, Jun. 2018, pp. 1–5.
[31] F. Cheng, S. Zhang, Z. Li, Y. Chen, N. Zhao, F. R. Yu, and V. C. M. Leung, "UAV trajectory optimization for data offloading at the edge of multiple cells," *IEEE Trans. Veh. Technol.*, vol. 67, no. 7, pp. 6732–6736, Jul. 2018.
[32] U. Challita, W. Saad, and C. Bettstetter, "Deep reinforcement learning for interference-aware path planning of cellular-connected UAVs," in *Proc. IEEE Int. Conf. Commun. (ICC)*, May 2018, pp. 1–7.
[33] H. C. Nguyen, R. Amorim, J. Wigard, I. Z. Kovács, T. B. Sørensen, and P. E. Mogensen, "How to ensure reliable connectivity for aerial vehicles over cellular networks," *IEEE Access*, vol. 6, pp. 12304–12317, 2018.
[34] M. Cui, G. Zhang, Q. Wu, and D. W. K. Ng, "Robust trajectory and transmit power design for secure UAV communications," *IEEE Trans. Veh. Technol.*, vol. 67, no. 9, pp. 9042–9046, Sep. 2018.
[35] G. Zhang, Q. Wu, M. Cui, and R. Zhang, "Securing UAV communications via joint trajectory and power control," *IEEE Trans. Wireless Commun.*, vol. 18, no. 2, pp. 1376–1389, Feb. 2019.
[36] S. Yan, S. V. Hanly, I. B. Collings, and D. L. Goeckel, "Hiding unmanned aerial vehicles for wireless transmissions by covert communications," in *Proc. IEEE Int. Conf. Commun. (ICC)*, May 2019, pp. 1–6.
[37] M. Chen, M. Mozaffari, W. Saad, C. Yin, M. Debbah, and C. S. Hong, "Caching in the sky: Proactive deployment of cache-enabled unmanned aerial vehicles for optimized quality-of-experience," *IEEE J. Sel. Areas Commun.*, vol. 35, no. 5, pp. 1046–1061, May 2017.
[38] T. Hou, Y. Liu, Z. Song, X. Sun, and Y. Chen, "Multiple antenna aided NOMA in UAV networks: A stochastic geometry approach," *IEEE Trans. Commun.*, vol. 67, no. 2, pp. 1031–1044, Feb. 2019.
[39] H. Wang, J. Wang, G. Ding, L. Wang, T. A. Tsiftsis, and P. K. Sharma, "Resource allocation for energy harvesting-powered D2D communication underlaying UAV-assisted networks," *IEEE Trans. Green Commun. Netw.*, vol. 2, no. 1, pp. 14–24, Mar. 2018.
[40] Y. Zhou, P. L. Yeoh, H. Chen, Y. Li, R. Schober, L. Zhuo, and B. Vucetic, "Improving physical layer security via a UAV friendly jammer for unknown eavesdropper location," *IEEE Trans. Veh. Technol.*, vol. 67, no. 11, pp. 11280–11284, Nov. 2018.
[41] L. Wirth, P. Oettershagen, J. Ambühl, and R. Siegwart, "Meteorological path planning using dynamic programming for a solar-powered UAV," in *Proc. IEEE Aerosp. Conf.*, May 2015, pp. 1–11.
[42] D. B. West, *Introduction to Graph Theory*. Upper Saddle River, NJ, USA: Prentice-Hall, 2000.
[43] M. Mozaffari, W. Saad, M. Bennis, Y.-H. Nam, and M. Debbah, "A tutorial on UAVs for wireless networks: Applications, challenges, and open problems," *IEEE Commun. Surveys Tuts.*, vol. 21, no. 3, pp. 2334–2360, Mar. 2019.
[44] F. Wu, D. Yang, L. Xiao, and L. Cuthbert, "Energy consumption and completion time tradeoff in rotary-wing UAV enabled WPCN," *IEEE Access*, vol. 7, pp. 79617–79635, 2019.
[45] Y. Zeng, J. Xu, and R. Zhang, "Energy minimization for wireless communication with rotary-wing UAV," *IEEE Trans. Wireless Commun.*, vol. 18, no. 4, pp. 2329–2345, Apr. 2019.
[46] M. Alzenad, A. El-Keyi, F. Lagum, and H. Yanikomeroglu, "3-D placement of an unmanned aerial vehicle base station (UAV-BS) for energy-efficient maximal coverage," *IEEE Wireless Commun. Lett.*, vol. 6, no. 4, pp. 434–437, Aug. 2017.
[47] P. K. Agarwal, N. Kumar, S. Sintos, and S. Suri, "Computing shortest paths in the plane with removable obstacles," in *Proc. 16th Scandin. Symp. Workshops Algorithm Theory*, vol. 101, 2018, pp. 5:1–5:15.

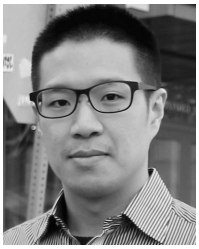

YU-JIA CHEN received the B.S. and Ph.D. degrees in electrical engineering from National Chiao Tung University, Taiwan, in 2010 and 2015, respectively. From 2015 to 2018, he was a Postdoctoral Research Fellow with National Chiao Tung University, Taiwan, and with Harvard University, from 2018 to 2019. In 2019, he joined National Central University, Taiwan, where he is currently an Assistant Professor with the Department of Communication Engineering. He has published more than 30 articles in peer-reviewed journal and conference papers. He holds four U.S. patents and four ROC patents. His research interests include low-latency communications, wireless sensing, and network security.

DA-YU HUANG received the B.S. degree in electrical engineering from National Chi Nan University, Taiwan, in 2018. He is currently pursuing the M.S. degree in communication engineering with the National Central University, Taiwan. His current research interests include wireless networks and machine learning.